ISSN 1028-334X, Doklady Earth Sciences, 2007, Vol. 415A, No. 6, pp. 922–925. © Pleiades Publishing, Ltd., 2007.
Original Russian Text © N.S. Bortnikov, T.L. Evstigneeva, N.V. Trubkin, 2007, published in Doklady Akademii Nauk, 2007, Vol. 415, No. 5, pp. 658–662.

GEOCHEMISTRY

Structural Features of ZnS from Modern Submarine Sulfide Ores of the Manus Basin (Pacific Ocean): Results of Electron Microscope Study

Corresponding Member of the RAS N. S. Bortnikov, T. L. Evstigneeva, and N. V. Trubkin

Received March 16, 2007

DOI: 10.1134/S1028334X07060219

In spite of a great number of publications, the formation and transformation of ZnS polytypes have not yet been clarified. Most researchers believe that the formation of the synthetic zinc sulfide polytype is related to solid-phase transformation of the 2*H* structure during cooling [1, 2]. However, detailed structural data on natural zinc sulfide typically represented by a mixture of polytypes are insufficient for making comparison and definite conclusions.

The features of the fine structure of natural ZnS are required for understanding its formation conditions. They are studied by various methods, such as X-ray diffractometry, electron paramagnetic resonance, electron diffraction, and electron microscopy. Evidently, reliable results can be obtained only by choosing the appropriate objects. Such objects are modern sulfide ores forming on the ocean floor, because they typically contain both ZnS modifications (sphalerite and wurtzite) and were not affected by metamorphic alterations.

Sulfides taken from unmetamorphosed sulfide mounds from the Manus back-arc basin [3–6] were studied using the TEM method to reveal specific features of zinc sulfides.

Sphalerite and wurtzite are the major ore minerals in a number of active and inactive chimneys. In some samples (2255-15, TM -1, TM-2, and TM-3), zinc sulfide is represented by relatively coarse-grained dendritelike aggregates of elongated (or equant) optically anisotropic grains with hexagonal habit. Other samples (2255-10) contain equant fine-grained crystals ZnS and nodular rims overgrowing chalcopyrite.

The study was performed in a JEM-100C JEOL transmission electron microscope equipped with EDS Kevex 5100. Material for suspension specimens was extracted from a polished thin section under optical microscope. Using a goniometer, ZnS particles were oriented in suspension along the (01.0)* plane of wurtzite or the (100)* plane of sphalerite to record the mutual orientation of crystals [10 $\bar{1}$0] (0001)//[10 $\bar{1}$1](111). X-ray patterns in these sections contain spots and alternating bands (line-reflections) of different intensities, which correspond to diagnostic series of reflections *h*0.1.* The character of lines depends on the local orientation, thickness, and focusing of crystal zones. Since the microscope resolution was too low (~10 Å) to obtain a direct two-dimensional image of the crystal lattice, the medium magnifications (~100 000 X) were applied. This allowed us to recognize ZnS polytypes with $c > 18$ Å using the periodicity of contrast line alternation in the images. The distribution of reflections in the diffraction images (*a***c**) and intervals of line contrast indicates that the sample contains an extremely long-periodic polytype or a combination of several polytypes with lower *c* parameters. The multiplicity of packing arrangement of polytype (*c*, unit cell height) and point symmetry were determined by the method of Verma and Krishna [7].

ZnS in samples TM-2 and TM-3 is represented by both perfect crystals of sphalerite and wurtzite and their disordered varieties with thin lamellae of long-periodic polytypes (Fig. 1). The weak point reflections 00.1 and *h*0.1 between 2*H* reflections indicate either definite regularity in the distribution of packing defects, which produces interlayers with longer periodicity polytypes, or the presence of randomly distributed defects in the perfect long-periodic polytype. The distribution of reflections in the diffraction patterns (*a***c**) and the range of line contrast indicate that sample TM-2 has a 3*C* structure. However, some domains consist of polytype 15R, particles with 8- and 6-layer packing, and structure 32 *L* (Fig. 1c). Individual defects are noted in the relatively large crystals and microtwinned intergrowths of ZnS with disordered sphalerite structure (TM-3) (Figs. 1a, 1b). Individual ZnS crystals have a randomly disordered

Institute of Geology of Ore Deposits, Petrography, Mineralogy, and Geochemistry, Russian Academy of Sciences, Staromonetnyi per. 35, Moscow, 119017 Russia; e-mail: bns@igem.ru

* Long-periodic polytypes occasionally yield line contrast in the direct images of nodal planes (0001).

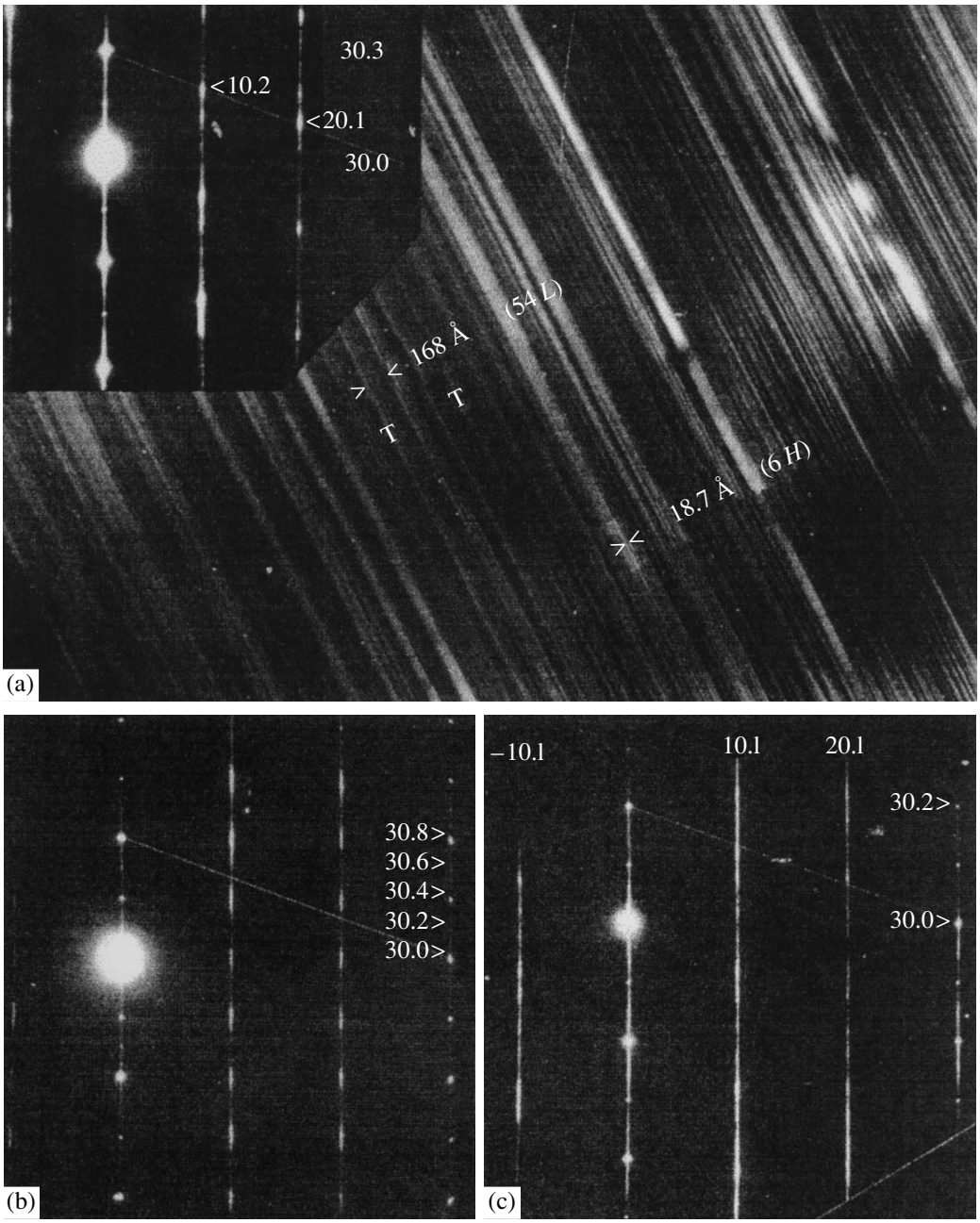

Fig. 1. Samples from the Manus basin. (a) TM-3, direct image (banded contrast) of nodal planes of the ZnS single crystals lattice composed of different polytypes; inset shows the SAED image of cubic or rhombohedral crystal (hexagonal cell indices are shown) with blocks of 6*H* and longer-periodicity (54*L*) structures; (b) TM-3, SAED image of crystal with periodically repeated structure 8*L*; (c) TM-2, diffraction pattern of crystal composed of long-periodic polytypes (for example, 12*R*, 15*R*); reference line shows the reflection shift.

wurtzite structure. Some microdiffraction patterns occasionally demonstrate superstructure reflections corresponding to the trigonal structure consisting of 15 and more layers, as well as a regular 8-layer (8*L*) (Fig. 1b) or rhombohedral 12-layer (12*R*) structure (Fig. 1c).

Images of nodal planes of lattice (0001) obtained at medium magnifications show that some crystals contain intergrowths of ZnS particles with different periods and packing arrangements of ZnS.

Most ZnS particles from sample M-15 have an intermediate structure between the sphalerite structure distorted by numerous hexagonal lamellae (30–35 Å thick) and a strongly disordered wurtzite structure. Sphalerite crystals from 0.005 to 0.02 μm in size have a microblock structure and consist of mutually disoriented crystallites (mosaic blocks) with the angle of relative disorientation of the grains around the ⟨111⟩ axes up to ≈2°. The structure of wurtzite single crystals changes from almost ideal 2*H* to a variety completely

disordered along axis *c* with the constant presence of layers with cubic packing. The same sample contains two particles with a perfect wurtzite lattice that is distorted only by some reflections.

ZnS from both active and healed chimneys from the ledge top of the main chimney (M-10/6a, 6b) has a sphalerite structure. It consists of aggregates of finely dispersed (gel-like) crystals with high Fe content and perfect or single crystals polysynthetically twinned along planes {111}.

The results obtained indicate that the studied natural ZnS is characterized by more diverse structural characteristics as compared to synthetic ones. There are crystals of individual structural modifications and intergrowths of different polytypes. Synthetic ZnS typically represents the intergrowths of different polytypes from one polytype group with the Ramsdel symbol *mH*-3*mR*, where m is an even number. The formation of almost all synthetic polytypes ZnS from gas phase or melt is consistent with the deformation mechanism. During solid-phase transformation related to cooling, the periodicity in the arrangement of basis layers is related to the movement of partial dislocations along the screw dislocation spiral, which leads to the formation of packing defect between structural layers. It is believed that the screw dislocation arises in the initial crystal with already imperfect layer packing. Therefore, the appearance of a new ZnS polytype depends on the starting structure [1, 2].

Natural crystals of ZnS often pertain to the same polytype species, while intergrowths can consist of any polytype combination. The absence of screw dislocations in all the studied samples rules out the solid-phase formation of ZnS polytypes. Samples of natural ZnS also differ from synthesized crystals in some other characteristics [1]. These observations indicate that natural ZnS polytypes were formed by chemical reactions from a hydrothermal solution. In nature, the formation of aggregates of ZnS polytypes is presumably provided by dislocation-free layer-by-layer growth, with some defects of layer packing. This results in a random packing arrangement with a period of only a few unit cells, because the same defect depending on the starting structure led to the formation of different polytypes.

The formation of distinct ZnS structures can be explained by different reasons. Since wurtzite has a deficiency of sulfur as compared to sphalerite [8], the Zn/S ratio in ZnS varies with change of fs_2 and temperature. According to [9], the cubic to hexagonal transformation and local accumulation of disordered *ccp–hcp* defects in natural sphalerite are caused by sulfur deficiency. Twinned boundaries [111] that were formed in sphalerite during growth are characterized by sulfur deficiency and high contents of Fe, O, and Mn [10]. The 2*H* wurtzite structure is characterized by sulfur vacancies, whereas 3*C* sphalerite must have zinc vacancies.* In response to a decrease in the metal/nonmetal ratio, the metallic atom configuration in the structure changes from hexagonal to cubic through introduction of a packing defect in the metallic layer. The higher the deviation of the metal/nonmetal ratio from unity, the closer the packing defects.

In addition to nonstoichiometry, the following factors affect the structure and growth of the crystals: (a) ratio of components in the solution; (b) temperature; (c) growth rate; (d) concentration of admixtures; and (e) size of ZnS crystallites. As is known, the temperature increase causes an increase in the number of more ordered crystals. The crystal growth rate (high oversaturation) has a positive correlation with the fraction of crystals with disordered structure. Increase of the Fe content in sphalerite facilitates decrease of the temperature of sphalerite–wurtzite transformation [12]. However, as to ZnS from the Manus basin, the Fe admixture presumably was not affected by crystallization (nucleation and growth) of ZnS, because the Fe content is significant in both sphalerite and wurtzite (sample M-15).

Though low-pressure wurtzite is stable at low pressure temperatures higher than 1200°C, sphalerite–wurtzite transformation in hydrothermal experiments occurs already at 225°C, which indicates wurtzite stability at these conditions. As is known, the free energy of small and large particles is different. If the surfaces of polymorphs of the same material have different values of free energy, the decrease in particle size is accompanied by a change in phase stability. This explains the higher stability of ZnS nanoparticles (size 3 nm) with hexagonal wurtzite structure at room temperature relative to the sphalerite structure [13]. The sphalerite cannot transform into wurtzite if the particle size does not exceed 3 nm. If the particle size is ~7 nm, wurtzite is converted into sphalerite at just 25°C. The HREM study showed that polygranular samples lack pure wurtzite, because it grows only at the surface of granular sphalerite particles. The wurtzite growth ceases when the size of the sphalerite–wurtzite surface approaches 22 nm [14].

The structure of ZnS particles depends not only on their size but also on the environment (presence of water and admixtures). Under hydrothermal conditions at room temperature, the structural configuration of ZnS particles approaches the sphalerite structure as the result of the reductive distortion of the surface and internal structure owing to ZnS–water bonding and S–H interaction [15]. According to Krishtabu, the presence of Cl and Ga in the solution decreases the temperature of sphalerite–wurtzite transformations and promotes the crystal growth.

The "Vienna Woods" sulfide chimneys are considered to form in sharply disequilibrium conditions [3, 5]. Coarse-grained sphalerite of the Vienna Woods ore field is presumably a secondary mineral, which crystallized from gels formed at the stage of saturation of loose anhydrite crusts with fluids. The deposition tem-

* A similar stoichiometric distortion was found in the polytypes SiC [11]: the Si/C ratio decreases with increase of layers with near-hexagonal packing.

perature of these sulfide chimneys is too low (~270°C or less [6]) for diffusion-controlled solid phase transformation. Therefore, sphalerite was presumably transformed through chemical redeposition of primary gel-like ZnS. This process was accelerated by subsequent heating of the massive sulfide–anhydrite chimney by hot hydrothermal solutions due to its screening from cold seawater [3].

A significant difference in the size and structure of sphalerite crystals from the top of the main chimney terrace (M-10/6a, b) of the Manus field could indicate its two-phase crystallization. Finely dispersed sphalerite precipitated from the oversaturated solution owing to sharp cooling of fluid at the contact with cold seawater. This caused a rapid growth of equant ZnS microcrystals in numerous nucleation centers. With accumulation and conservation, the gel-like sphalerite was recrystallized into twinned crystals due to the delivery of micropore solutions during the stage of "pipe" extinction.

The features of sphalerite single crystals in the high-temperature White Spire field (southeastern margin of the Vienna Woods) indicate wurtzite–sphalerite transformation, because crystallization of sphalerite from the solution cannot produce the packing defect that normally intersects several sphalerite grains. ZnS was initially precipitated as well-crystallized wurtzite (with individual packing defects) and/or its disordered variety. Wurtzite is converted into sphalerite due to change in thermodynamic conditions (*p, T*) or environmental chemistry (pH, fs_2). According to experiments [8], this transformation is much more rapid than the opposite one, because the sphalerite–wurtzite activation energy is significantly lower than that for the opposite transformation. The packing defects in wurtzite are responsible for the formation of cubic sphalerite lamellae and favorable for reduction in the activation energy of nucleation. The environmental changes lead to dissolution of the wurtzite phase. As soon as the cubic layer stable in these conditions is formed, the epitaxial nucleation of sphalerite begins at this layer. Along this interlayer, the matrix is dissolved simultaneously and a new phase grows without significant migration of the matter. The redeposition of the matter in this way leads to the formation of mosaic sphalerite monocrystal, individual areas of which exceed only several times the stable germ size (about 0.005 μm) upon preservation of relict cubic-structured layers.

CONCLUSIONS

1. ZnS from the Manus basin is represented by micron- and submicron-sized sphalerite crystals with perfect cubic structure distorted only by some packing defects.

2. The presence of mutually oriented fine-grained sphalerite aggregates in the Manus ore field reflects the change of physicochemical conditions during formation of sulfide chimneys and could support the assumption of rhythmic formation of hydrothermal deposits.

3. The different degree of ordering–disordering in layer packing and intergrowths of long-periodic polytypes in zinc sulfide crystals from the Manus ore occurrences (samples TM) indicate disequilibrium environmental conditions during crystal growth.

4. The phase stability of ZnS is determined by the nanodimension of the newly forming particles and the presence of H_2O and Cl in the mineral-forming environment.

REFERENCES

1. I. I. Steinberger, *Crystal Growth and Characterization of Polytype Structures* (Pergamon Press, Oxford, 1983), Vol. 7, pp. 7–53.
2. S. Mardix, Bull. Miner. **109**, No. 1/2, 131 (1986).
3. A. P. Lisitsyn. K. Kruk, Yu. A. Bogdanov, et al., Izv. Ross. Akad. Nauk, Ser. Geol., No. 10, 34 (1992).
4. T. N. Shadlun, N. S. Bortnikov, Yu. A. Bogdanov, et al., Geol. Rudn. Mestorozhd. **34**, 3 (1992).
5. N. S. Bortnikov and A. P. Lisitsyn, in *Geology and Mineral Resources of the World Ocean* (VNIIOkeanologiya, Moscow, 1995), pp. 158–173 [in Russian].
6. N. S. Bortnikov, V. A. Simonov, and Yu. A. Bogdanov, Geol. Ore Dep. **46**, (2004) [Geol Rudn. Mestorozhd. **46**, 74 (2004)].
7. A. Verma and P. Krishna, *Polymorphism and Polytypism in Crystals* (John Wiley, New York, 1966; Mir, Moscow, 1969).
8. S. D. Scott and H. L. Barnes, Geochim. Cosmochim. Acta **36**, 1275 (1972).
9. M. Akizuki, Am. Mineral. **66**, 1000 (1981).
10. V. Srot, A. Recnik, C. Scheu, S. Sturm, and B. Mirtic, Am. Mineral. **88**, 1809 (2003).
11. Y. M. Tairov and V. F. Tsvetkov, J. Cryst. Growth **52**, 146 (1981).
12. St. Knitter and M. Binnewies, Z. Anorg. Allg. Chem. **625**, 1582 (1999).
13. H. Zhang and J. F. Banfield, Nano Lett. **4**, 713 (2004).
14. F. Huang and J. F. Banfield, J. Am. Chem. Cos., No. 12, 4523 (2005).
15. H. Zhang, F. Huang, B. Gilbert, and J. F. Banfield, J. Phys. Chem. **107**, 13051 (2003).